

ORIGINAL ARTICLE OPEN ACCESS

2-Methoxyestradiol Inhibits the Oxygen-Sensing Pathway in Keloid Fibroblasts by Targeting HIF-1 α /PHD

Ming-Zi Zhang^{1,2} | Zhi-Jin Li^{1,2} | Wen-Bo Xia³ | Lou-Bin Si^{1,2} | Nanze Yu^{1,2} | Xiao-Jun Wang^{1,2}  | Xiao Long^{1,2}

¹Department of Plastic Surgery, Peking Union Medical College Hospital, Beijing, China | ²Center for Regenerative Medicine & Plastic Surgery Research, Peking Union Medical College Hospital, Beijing, China | ³Department of Orthopedics, Qingdao Huangdao District Hospital of Traditional Chinese Medicine, Qingdao, China

Correspondence: Xiao-Jun Wang (pumchwxj@163.com) | Xiao Long (pumclongxiao@126.com)

Received: 1 September 2024 | **Revised:** 1 March 2025 | **Accepted:** 10 March 2025

Funding: This work was supported by National Natural Science Foundation of China (82102326); Peking Union Medical College Hospital Young Reserve Talent Development Program (UHB12264); National High Level Hospital Clinical Research Funding (2022-PUMCH-B-041).

Keywords: 2-Methoxyestradiol | fibroblast | keloid | oxygen-sensing pathway

ABSTRACT

Maintaining oxygen homeostasis is a basic cellular process for adapting to physiological oxygen variations in which the oxygen-sensing pathway plays a critical role, especially in tumour progression. Little is known about the activity of the oxygen-sensing pathway in keloid tissue. In this study, key features of the oxygen-sensing pathway and its downstream effects were evaluated and compared between normal skin tissue and keloid tissue. Keloid tissue showed increased oxygen-sensing pathway activation and a higher expression of key downstream factors such as tumour necrosis factor-1 α (TNF- α) and vascular endothelial growth factor (VEGF). In addition, the effects of 2-methoxyestradiol on the oxygen-sensing pathway in both hypoxic and normoxic keloid fibroblasts were evaluated. Our results suggest that 2-methoxyestradiol could be used to inhibit keloid fibroblast activity by inhibiting the oxygen-sensing pathway and its downstream effectors.

1 | Introduction

Oxygen metabolism is a fundamental biological step for all vertebrate organisms. The mechanism by which cells sense oxygen to initiate metabolism remained unclear until the 1990's. Drs. Gregg Semenza, William Kaelin and Peter Ratcliffe discovered an oxygen-sensing pathway in mammalian cells that addressed this fundamental gap in knowledge and were awarded the 2019 Nobel Prize in Physiology or Medicine [1]. Oxygen-sensing pathway activation leads to many downstream effects via several effectors, such as angiogenesis (vascular endothelial growth factor, [VEGF]) [2], collagen generation (Collagen I, Collagen III) [3], inflammation (tumour necrosis factor-1 α , [TNF- α]) [4] and apoptosis (Bcl-2, Bax) [5].

Keloids, benign skin tumours, are caused by cutaneous injury and irritation, including trauma, insect bites, burns, surgery, vaccination, skin piercings, acne, folliculitis, chicken pox and herpes zoster infection [6]. Previous studies have shown that keloid tissue is a hypoxic microenvironment with high expression of hypoxia inducible factor-1 α (HIF-1 α) [7]. By applying the oxygen-sensing pathway theory, we reveal here the activation level of the oxygen-sensing pathway and its downstream effectors in keloid tissue.

2-Methoxyestradiol (2ME2) is a promising new chemotherapeutic that exhibits anti-tumour effects by inhibiting cell proliferation and inducing apoptosis in a variety of malignant cell lines [8, 9]. In our previous studies, 2ME2 showed therapeutic potential for treating keloids [10, 11] by inhibiting

Ming-Zi Zhang and Zhi-Jin Li—co-first author.

This is an open access article under the terms of the [Creative Commons Attribution-NonCommercial](https://creativecommons.org/licenses/by-nc/4.0/) License, which permits use, distribution and reproduction in any medium, provided the original work is properly cited and is not used for commercial purposes.

© 2025 The Author(s). *International Wound Journal* published by Medicalhelplines.com Inc and John Wiley & Sons Ltd.

Summary

- Keloid, known as a benign tumour, seriously affected patients' life quality.
- Oxygen plays an important role in keloid progress.
- In this study, the oxygen-sensing pathway was assessed in keloid tissue, and the inhibiting effect and mechanism of 2-Methoxyestradiol towards keloid fibroblasts was also investigated. According to the results, the oxygen-sensing pathway was highly activated in keloid tissue; 2-Methoxyestradiol could inhibit keloid progress by targeting HIF-1 α /PHD.
- 2-Methoxyestradiol also has a positive effect towards the downstream factors of the oxygen-sensing pathway, such as inhibiting angiogenesis, regulating collagen generation and inflammation and promoting apoptosis levels.

angiogenesis, collagen generation, and inflammation and by promoting apoptosis. Because these processes are downstream effects of the oxygen-sensing pathway, we further investigated the mechanism by which 2ME2's affects the pathway in keloid fibroblasts.

2 | Materials and Methods

2.1 | Patient Selection

From July 2022 to June 2023, 20 patients (ranging in age from 20 to 47 years old; Median age: 34.5 years old) were randomly selected from the Department of Plastic Surgery. Ten patients were keloid patients (gender ratio 1:1; Median age: 34.5 years old) and 10 were non-keloid patients (gender ratio 1:1; Median age: 34 years old). All keloid cases were caused by chest trauma and diagnosed by pathological examination. All patients declared no history of systemic disorders, recent drug use, or other treatments. The keloid patients and non-keloid patients showed no significant differences in age, gender, body mass index (BMI), or sample location.

2.2 | Tissue Sample Management and Fibroblast Culture

Tissue sample management and keloid fibroblast (from keloid patients) cell culture were performed according to previous protocols [10–12].

2.2.1 | Tissue Sample Management

The central part of the keloid and normal skin tissue was obtained for this study. Tissue samples were washed in phosphate-buffered saline (PBS) after removing fat tissue and hair. Samples were divided into two parts for further experiments. Samples for staining were placed in a 10% formalin solution for 48 h and embedded in paraffin. Other samples were used for protein extraction and quantitative expression analysis.

2.2.2 | Fibroblast Culture

Keloid samples were cut into 0.2–0.3 cm³ blocks and laid onto 75 cm² culture flasks. In total, 10 mL of Dulbecco's minimal essential medium (Gibco, Big Cabin, OK, USA) supplemented with 10% fetal bovine serum (Gibco), penicillin (100 U/mL), and streptomycin (100 μ g/mL, Gibco) was added to the flasks after 4 h of tissue adherence. Flasks were kept at 37°C in a 5% carbon dioxide-enriched, humidified atmosphere. Culture medium was changed every 3 days. Normal skin fibroblast cell culture was conducted according to Vangipuram [13].

2.3 | Grouping and Drug Intervention

Tissue experiment: Tissue samples were divided into two groups: (1) N group—normal skin tissue; (2) K group—keloid tissue.

Cell experiment: Keloid fibroblasts were cultured in a hypoxic environment (1% oxygen, 5% carbon dioxide, 94% nitrogen) or a normoxic environment (21% oxygen, 5% carbon dioxide, 74% nitrogen). Keloid fibroblasts were divided into 10 groups: (1) Hypoxic K: keloid fibroblasts cultured in a hypoxic environment; (2) Hypoxic K + 2ME2: keloid fibroblasts treated with 2ME2; (3) Hypoxic K + DMSO: keloid fibroblasts treated with dimethyl sulfoxide (DMSO); (4) Hypoxic K + VH298: keloid fibroblasts treated with Von Hippel–Lindau inhibitor (VHL inhibitor VH298); (5) Hypoxic K + TP0463518: keloid fibroblasts treated with a prolyl hydroxylase inhibitor (PHD inhibitor TP0463518); (6) Hypoxic K + VH298 + 2ME2: keloid fibroblasts treated with VH298 and 2ME2; (7) Hypoxic K + TP0463518 + 2ME2: keloid fibroblasts treated with TP0463518 and 2ME2; (8) Normoxic K: keloid fibroblasts cultured in a normoxic environment; (9) Normoxic K + 2ME2: keloid fibroblasts treated with 2ME2; (10) Normoxic K + DMSO: keloid fibroblasts treated with DMSO.

The drug concentrations used in the cell experiments were 6.975 μ M 2ME2 (in 0.07% DMSO) [9, 10], 0.07% DMSO, 50 nM VH298 (in 0.01% DMSO) and 20 nM TP0463518 (in 0.005% DMSO). All drugs were incubated with keloid fibroblasts for 24 h before further experimentation. All drugs were purchased from Selleck Chemicals (Houston, USA).

2.4 | Haematoxylin and Eosin (H&E) and Masson Staining

H&E and Masson staining were used to histologically characterise the N and K groups. For H&E staining, slides were dewaxed at 70°C for 30 min and washed twice in xylene for 15 min. Then, slides were rehydrated in an ethanol gradient for 15 min. Haematoxylin staining was done for 5 min, followed by a 10 s 1% hydrochloric acid treatment. Slides were washed with running water for 15 min. Eosin counterstain was done for 1 min. Dehydration was performed with an alcohol gradient. Slides were subsequently washed with xylene and mounted. In H&E staining, the red colour corresponds to the cytoplasm and other components, while the blue colour corresponds to the nuclei.

Masson staining was performed with a staining kit according to the manufacturer's instructions (Heart Biological Technology, Xian, China). In Masson staining, the red colour corresponds to cells, while the blue colour corresponds to fibrils.

2.5 | Western Blot Assessment

The Total Protein Extraction Kit (Bio-Rad Laboratories, CA, USA) was used for protein extraction from tissue (50mg) and fibroblasts. After 24 h of treatment, samples of fibroblasts were incubated in a cell lysis buffer (246 μ L of lysis buffer, 1.25 μ L of phosphatase inhibitor, 0.25 μ L of protease inhibitor and 2.5 μ L of phenylmethylsulfonyl fluoride [PMSF]) and centrifuged for 15 min (4°C, 14000 rpm). The supernatant proteins from 60 μ g of tissue or 30 μ g of fibroblasts were separated on a 10% SDS-PAGE gel. Immunoblotting was performed after transferring protein onto nitrocellulose membranes. After 2 h of membrane blocking with blocking buffer (Li-cor, Lincoln, USA), the membrane was incubated with anti-HIF-1 α , anti-HIF-1 β , anti-VEGF, anti-PHD, anti-TNF- α , anti-Collagen I, anti-Collagen III, anti-Bcl-2, anti-Bax, or anti-VHL primary antibodies in a humidified shaker overnight at 4°C. All primary antibodies were purchased from Abcam (USA). The ratio of primary antibodies was 1:500 (tissue) or 1:200 (fibroblasts). The membranes were incubated with secondary antibody (1:10000, Li-cor) for 1 h in the dark. Membrane scanning and data analysis was performed with a Double-colour infrared laser imaging system (Odyssey, Li-cor).

2.6 | Cell Activity Detection

Fibroblast activity was detected by a Cell Counting Kit-8 (CCK-8) assay according to the manufacturer's instructions (Dojindo, Kumamoto, Japan). Fibroblasts (5000 cells/well) were seeded in 96-well plates for 4 days. A microplate reader was used to measure the optical density at 450 nm every 24 h.

2.7 | Statistical Analysis

All data are presented as the mean \pm standard deviation (mean \pm SD) and analysed by SPSS Statistics 24.0 software (SPSS Inc., IL). The independent sample *t* test was used for tissue experiment data analysis. One-way analysis of variance (ANOVA) and the least significant difference (LSD) *t*-test were used for

fibroblast experiment data analysis. *p* < 0.05 was considered statistically significant.

3 | Results

3.1 | Patient Information

Twenty patients were involved in this study, including 10 keloid patients and 10 non-keloid patients. The average keloid patient age was 32.70 \pm 7.82 years and 35.50 \pm 5.19 years for non-keloid patients. The average keloid patient BMI was 22.20 \pm 3.22 kg/m² and 23.76 \pm 2.12 kg/m² for non-keloid patients. There was no significant difference in age or BMI between the keloid patients and non-keloid patients (Table 1).

3.2 | Morphological and Histological Observations by H&E and Masson Staining

H&E and Masson staining images are shown in Figure 1. Compared with normal skin tissue, the keloid tissue had denser and more disordered collagen fibrils. In contrast, looser fibrils were observed in normal skin tissue. In addition, more infiltrating cells were seen in the keloid tissue.

3.3 | Protein Expression Levels in Tissue

Quantitative analysis of tissue protein expression levels was measured by Western blot. Oxygen-sensing pathway proteins and downstream effector proteins were measured in normal and keloid tissue (Figure 2 and Table S1). Compared with normal skin tissue, HIF-1 α , HIF-1 β and PHD expression was significantly higher in keloid tissue; however, VHL expression was significantly decreased. The expression of downstream effectors of the oxygen-sensing pathway such as VEGF, TNF- α , Collagen I, Collagen III and Bcl-2 was much higher in keloid tissue. Bax expression in keloid tissue was lower than in normal skin tissue. All differences were statistically significant.

3.4 | Keloid Fibroblast Activity After Drug Treatment

Four days of hypoxic and normoxic keloid fibroblast cell activity are shown in Figure 3 and Table S2. Fibroblast activity

TABLE 1 | Basic information of all patients.

| Items | | Group | |
|--------------------------|-------------|------------------|---------------------|
| | | Keloid patients | Non-keloid patients |
| Age (years) | Median Age | 34.5 | 34 |
| | Average Age | 32.70 \pm 7.82 | 35.50 \pm 5.19 |
| Gender | Female | 5 | 5 |
| | Male | 5 | 5 |
| BMI (kg/m ²) | | 22.20 \pm 3.22 | 23.76 \pm 2.12 |
| Sample location | | Chest region | Chest region |

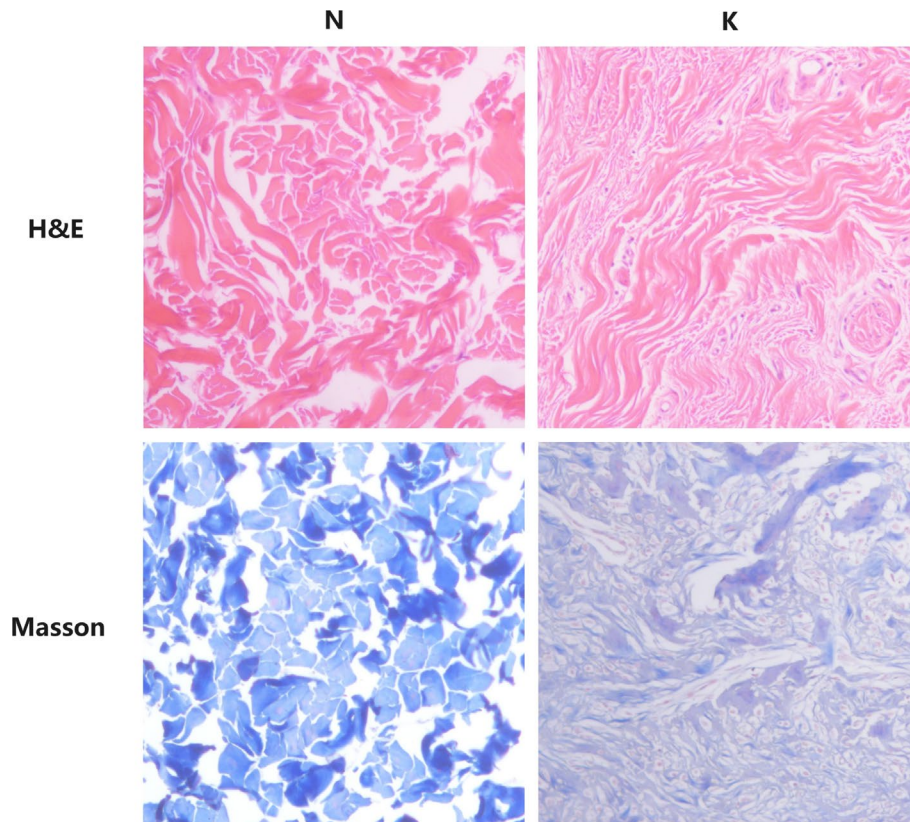


FIGURE 1 | The histological image of Haematoxylin and eosin (H&E) staining and of Masson staining in N group and K group (400×). Both in H&E and Masson staining images, keloid tissue showed more dense and disordered arrayed collagen fibrils with more infiltrated cells.

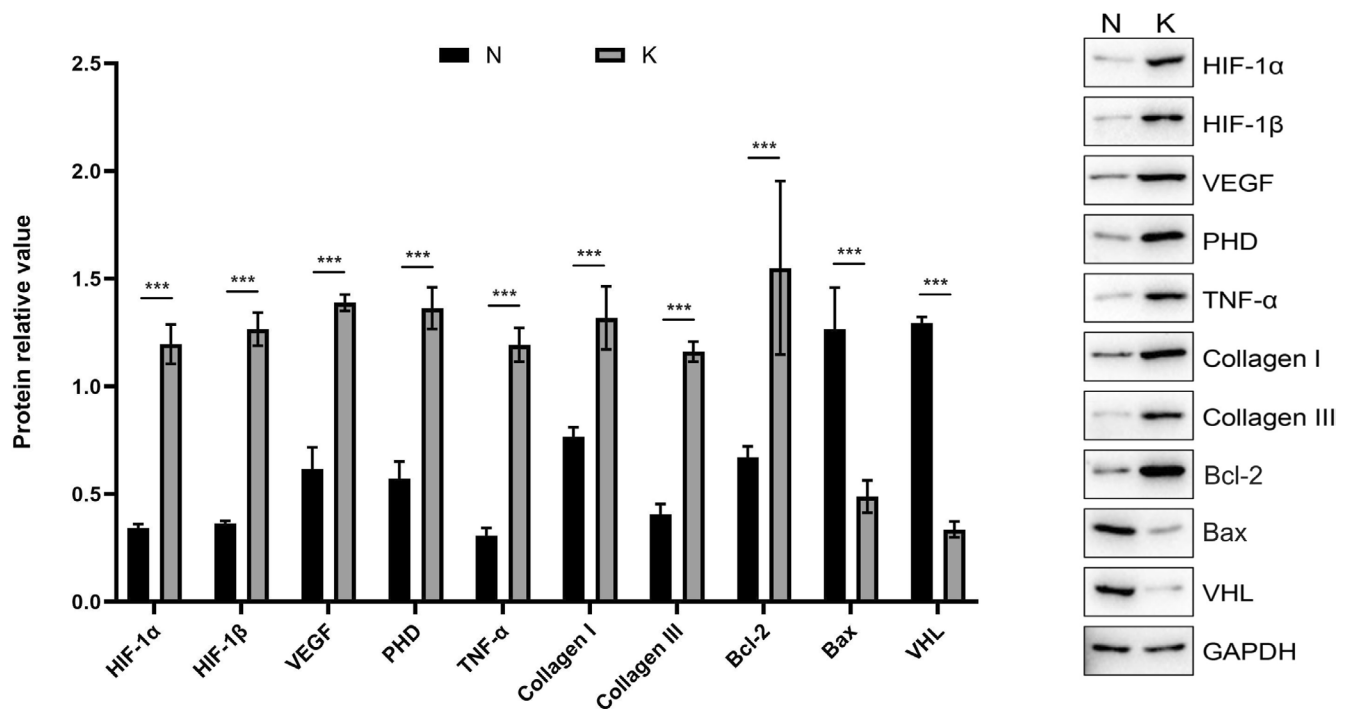


FIGURE 2 | Protein expression of target factors in tissue level. Compared with the N group, protein expression of all target factors (except VHL and Bax) were increased remarkably in the K group. Values are shown as means \pm SD ($n=10$ in each group; *** $p<0.001$).

increased with time after one drug intervention. On Day 1, there were significant differences between the hypoxic and normoxic groups. On Day 2, additional differences between the groups were observed. On Day 3, fibroblast activity was inhibited by

2ME2 in the hypoxic environment. On Day 4, 2ME2 inhibited fibroblast activity in both hypoxic and normoxic environments. The DMSO vehicle control did not induce significant changes in either the Hypoxic or Normoxic K cells. On Day 4,

fibroblasts reached the highest cell activity of all groups after treatment with VH298. However, this effect was significantly inhibited by 2ME2. Cell activity in the Hypoxic K and Hypoxic K+TP0463518 groups showed no significant differences. 2ME2 decreased Hypoxic K+TP0463518 cell activity. In all Hypoxic or Normoxic groups on Day 4, the lowest fibroblast cell activity occurred with the treatment of 2ME2 alone.

3.5 | Protein Expression Levels in Cells

Quantitative analysis of expression levels of oxygen-sensing pathway proteins and their downstream effectors was measured using Western blotting and is shown in Figure 4 and Table S3. Compared with the Normoxic K group, HIF-1 α , HIF-1 β , PHD, TNF- α , Collagen I, Collagen III and Bcl-2 expression were increased, and VHL and Bax expression were significantly decreased in the Hypoxic K group. VHL expression was significantly decreased by VH298 treatment, while PHD expression was significantly decreased by TP0463518 treatment. No significant differences were observed between the Hypoxic K and Hypoxic K + DMSO groups.

2ME2 treatment significantly decreased HIF-1 α and PHD expression and increased VHL expression in the Hypoxic K group. 2ME2 also decreased VEGF, TNF- α , Collagen I, Collagen III and Bcl-2 expression while increasing Bax expression.

Compared to the Hypoxic K+VH298 group, the addition of 2ME2 inhibited all key factors except Bax and VHL. Bax expression was significantly increased, while VHL expression showed no significant difference in expression in the Hypoxic K+VH298+2ME2 group. Compared to the Hypoxic K+TP0463518 group, the addition of 2ME2 inhibited all key factors except PHD, Bax and VHL. PHD, Bax and VHL expression were significantly increased in the Hypoxic K+TP0463518+2ME2 group.

4 | Discussion

Oxygen plays an essential role in numerous biological activities, with the ability to sense oxygen being a critical first step in metabolic processes. Advances in the field of oxygen research led to the discovery of an oxygen-sensing pathway that opened a new scientific field. This extraordinary discovery led to Drs. Gregg Semenza, William Kaelin and Peter Ratcliffe being awarded the Nobel Prize in Physiology or Medicine in 2019. Disorders of the oxygen-sensing pathway underpin numerous human diseases, such as inflammatory and cardiovascular conditions and cancer.

The oxygen-sensing pathway proceeds as follows [14]: In a hypoxic environment, HIF-1 (composed of HIF-1 α and HIF-1 β) expression increases significantly, and the protein is translocated to the nucleus, where it activates the oxygen-sensing pathway.

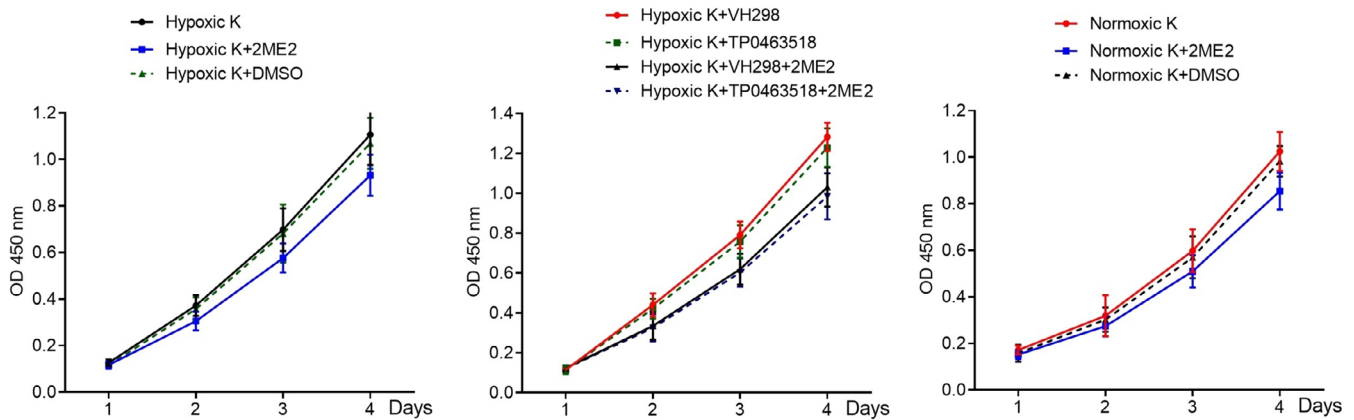


FIGURE 3 | Keloid fibroblasts activity in all the groups at different time points. Fibroblasts activity increased with time after once drug intervention.

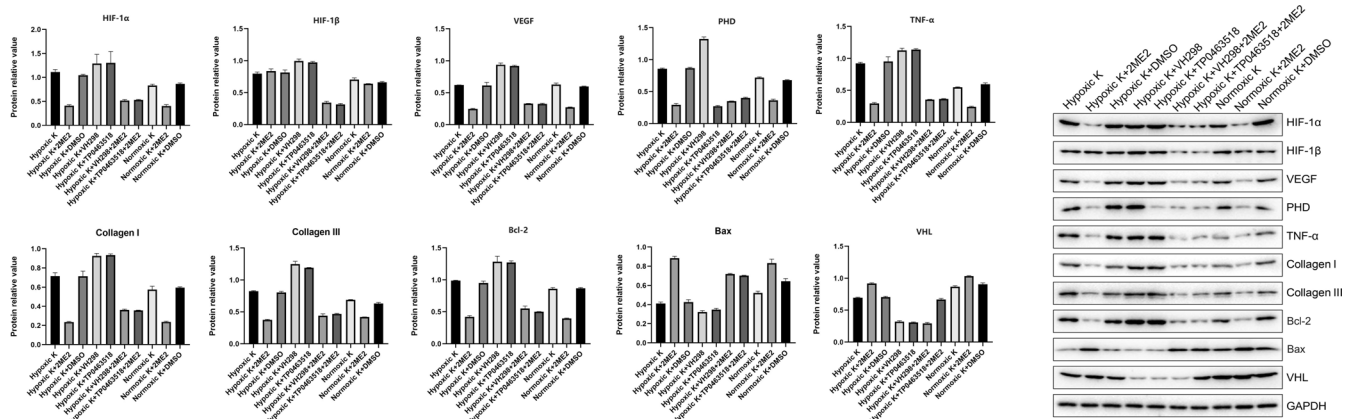


FIGURE 4 | Protein expression of target factors in cell level. Values are shown as means \pm SD ($n = 10$ in each group).

This leads to upregulation of proteins like VEGF that promote an adaptive response to hypoxia and subsequent angiogenesis, collagen generation, inflammation and apoptosis [15]. In a normoxic environment, HIF-1 α is hydroxylated by PHD using molecular oxygen as a substrate. The hydroxyl group allows VHL to interact with HIF-1 α and induces HIF-1 degradation.

Keloids form because of pathological wound healing after injury. Unlike hypertrophic scars, keloids tend to outgrow the original boundary of the wound without regression and are thus considered benign tumours [16]. Keloid tissue contains more densely packed and disordered collagen fibrils along with more infiltrated cells. Our results showed higher HIF-1 α , HIF-1 β and PHD expression and lower VHL expression in keloid tissue compared to normal tissue, indicating that the oxygen-sensing pathway was activated in keloid tissue. Although HIF-1 α is the essential regulator, HIF-1 α and HIF-1 β combine to form the heterodimeric HIF-1 protein as part of the oxygen-sensing pathway [17]. Because PHD acts as a direct oxygen sensor, it plays a pivotal role in regulating HIF-1 stability. Based on PHD's effect on HIF-1 α , we expected PHD expression to decrease. However, our data showed the opposite effect. Besides its ability to hydroxylate HIF-1 α , PHD reacts with reactive oxygen species (ROS), nitric oxide (NO) and certain metabolites [18]. Previous studies have demonstrated that excessive ROS and high NO levels are related to keloid formation [19, 20]. We therefore inferred that the higher PHD expression may be caused by high levels of ROS or NO. VHL, considered a tumour suppressor protein, inhibits HIF-1 α accumulation and translocation to the nucleus. HIF-1 α accumulation in keloid tissue leads to VHL consumption through other approaches [21, 22]. The expression of all downstream HIF-1 pathway effectors tested here, except Bax, was increased in keloid tissue. This explains the appearance of rich blood vessels and fibrils, high inflammation levels, and relatively low amounts of apoptosis in keloid tissue.

Oestrogens occurring naturally in the body are metabolised to catechol oestrogens (2- and 4-hydroxyestradiol) by the cytochrome P450 enzymes. 2-Hydroxy catechol oestrogens are further metabolised by catechol-O-methyltransferase to 2ME2, which has antiangiogenic and antitumor activities [23, 24]. Previous studies showed that 2ME2 inhibits cell growth and induces cell death in malignant cell lines such as breast cancer [25], melanoma [26] and prostate cancer lines [27]. In addition, 2ME2 also shows promising effects and potential applications in non-tumour diseases such as Parkinson's disease [28], pulmonary hypertension [29] and scleroderma [30]. Long first introduced 2ME2 to keloid research and showed that 2ME2 increases radiation-induced apoptosis of keloid fibroblasts by targeting HIF-1 α [31]. Our previous studies also showed that 2ME2 increases keloid fibroblast apoptosis through a caspase-dependent mechanism and inhibits keloid fibroblast proliferation by targeting p38 in the mitogen-activated protein kinase/extracellular signal-regulated kinase (MAPK/Erk) signalling pathway [10, 11]. Based on our tissue experiments, we sought to further investigate how 2ME2 affects the oxygen-sensing pathway in keloid fibroblasts.

Keloid fibroblast cell activity increased from Day 1 to 4. 2ME2 significantly inhibited keloid fibroblast cell activity, while 0.07% DMSO showed no significant inhibitory effect. DMSO was

used to solubilise the 2ME2 and is toxic at high concentrations. Though numerous studies have looked at how DMSO influences cells, the recommended concentrations to minimise toxicity are quite different. Most studies suggest a concentration below 0.2% [32, 33] to mitigate biological toxicity, and the concentrations used here were well below this upper limit. Furthermore, 2ME2 also inhibited cell activity after treatment with VHL or PHD inhibitors.

Key factors in the oxygen-sensing pathway changed in expression between the Hypoxic K group and Normoxic K group in fibroblast cells. This suggests that a hypoxic environment led to positive activation of the oxygen-sensing pathway in keloid fibroblasts. 2ME2 decreased HIF-1 α and PHD expression and increased VHL expression. When inhibiting PHD with TP0463518, 2ME2 still increased PHD expression, implying that 2ME2 may influence PHD in some way. 2ME2 showed an unobvious effect on VHL expression when inhibiting it with VH298. 2ME2 decreased the expression of downstream factors in the oxygen-sensing pathway such as VEGF, TNF- α , Collagen I, Collagen III and Bcl-2 while increasing Bax expression. 2ME2 inhibited angiogenesis and collagen generation, thereby ameliorating inflammation and promoting apoptosis.

Based on our results, we inferred that 2ME2 may be a promising and effective drug for keloid treatment. The poor water solubility of 2ME2 may limit its clinical application. However, local 2ME2 use may be a way to overcome this issue and ensure it is used at an effective concentration. Steroids are the first-line medication for treating keloids. Our former study's result [11] showed that the 50% inhibitory concentration of 2ME2 is quite lower than that of steroids (triamcinolone acetonide), which may reduce side effects in clinical application.

Our work only focused on the mechanistic effects of 2ME2 at the cellular level. Future work will involve animal experiments to further investigate 2ME2's promise as a novel keloid treatment.

5 | Conclusion

The oxygen-sensing pathway exists in keloid tissue and is activated or inhibited according to different oxygen concentrations. 2ME2 negatively activates the oxygen-sensing pathway by targeting HIF-1 α /PHD and could be a new drug to treat keloids in the context of dermatology and plastic surgery.

Ethics Statement

This study has been approved by the Bioethical Committee of Peking Union Medical College Hospital (I-24PJ0679). All patients signed informed consents and were not treated besides planned surgery.

Conflicts of Interest

The authors declare no conflicts of interest.

Data Availability Statement

The data that support the findings of this study are available from the corresponding author upon reasonable request.

References

1. C. Liao and Q. Zhang, "Understanding the Oxygen-Sensing Pathway and Its Therapeutic Implications in Diseases," *American Journal of Pathology* 190, no. 8 (2020): 1584–1595.
2. E. Nasyrov, K. A. Nolan, R. H. Wenger, et al., "The Neuronal Oxygen-Sensing Pathway Controls Postnatal Vascularization of the Murine Brain," *FASEB Journal* 33, no. 11 (2019): 12812–12814.
3. A. Bouthelie and J. Aragonés, "Role of the HIF Oxygen Sensing Pathway in Cell Defense and Proliferation Through the Control of Amino Acid Metabolism," *Biochimica et Biophysica Acta, Molecular Cell Research* 1867, no. 9 (2020): 118733.
4. J. Vinkel, B. Arenkiel, and O. Hyldegaard, "The Mechanisms of Action of Hyperbaric Oxygen in Restoring Host Homeostasis During Sepsis," *Biomolecules* 13, no. 8 (2023): 1228–1246.
5. R. Datta Chaudhuri, A. Banik, B. Mandal, et al., "Cardiac-Specific Overexpression of HIF-1 α During Acute Myocardial Infarction Ameliorates Cardiomyocyte Apoptosis via Differential Regulation of Hypoxia-Inducible Pro-Apoptotic and Anti-Oxidative Genes,".
6. R. Ogawa, "Keloid and Hypertrophic Scars Are the Result of Chronic Inflammation in the Reticular Dermis," *International Journal of Molecular Sciences* 18, no. 3 (2017): 606–615.
7. X. Ma, J. Chen, B. Xu, et al., "Keloid-Derived Keratinocytes Acquire a Fibroblast-Like Appearance and an Enhanced Invasive Capacity in a Hypoxic Microenvironment In Vitro," *International Journal of Molecular Medicine* 35, no. 5 (2015): 1246–1256.
8. M. Ba and Y. Duan, "Advance of 2-Methoxyestradiol as a Promising Anticancer Agent for Cancer Therapy," *Future Medicinal Chemistry* 12, no. 4 (2020): 273–275.
9. T. Namekawa, S. Kitayama, K. Ikeda, et al., "HIF1 α Inhibitor 2-Methoxyestradiol Decreases NRN1 Expression and Represses In Vivo and In Vitro Growth of Patient-Derived Testicular Germ Cell Tumor Spheroids," *Cancer Letters* 489 (2020): 79–86.
10. M. Z. Zhang, Y. F. Liu, N. Ding, et al., "2-Methoxyestradiol Improves the Apoptosis Level in Keloid Fibroblasts Through Caspase-Dependent Mechanisms In Vitro," *American Journal of Translational Research* 10, no. 12 (2018): 4017–4029.
11. M. Z. Zhang, Y. F. Liu, L. Ding, et al., "2-Methoxyestradiol Inhibits the Proliferation Level in Keloid Fibroblasts Through p38 in the MAPK/Erk Signaling Pathway," *Journal of Cosmetic Dermatology* 22, no. 11 (2023): 3135–3142, <https://doi.org/10.1111/jocd.15810>.
12. M. Z. Zhang, X. H. Dong, W. C. Zhang, et al., "A Comparison of Proliferation Levels in Normal Skin, Physiological Scar and Keloid Tissue," *Journal of Plastic Surgery and Hand Surgery* 57, no. 1–6 (2023): 122–128.
13. M. Vangipuram, D. Ting, S. Kin, et al., "Skin Punch Biopsy Explant Culture for Derivation of Primary Human Fibroblasts," *Journal of Visualized Experiments* 77 (2013): e3379–e3381.
14. J. W. Wilson, D. Shakir, M. Batie, et al., "Pxygen-Sensing Mechanisms in Cells," *FEBS Journal* 287, no. 18 (2020): 3888–3906.
15. C. B. Thompson, "Into Thin Air: How We Sense and Respond to Hypoxia," *Cell* 167, no. 1 (2016): 9–11.
16. I. Appleton, N. J. Brown, and D. A. Willoughby, "Apoptosis, Necrosis and Proliferation: Possible Implications in the Etiology of Keloid," *American Journal of Pathology* 149, no. 5 (1996): 1441–1447.
17. D. Flood and C. T. Taylor, "Targeting HIF-1 to Treat AML," *Nature Cancer* 5, no. 6 (2024): 821–822.
18. W. G. Kaelin, Jr. and P. J. Ratcliffe, "Oxygen Sensing by Metazoans: The Central Role of the HIF Hydroxylase Pathway," *Molecular Cell* 30, no. 4 (2008): 393–402.
19. X. Han, L. Ju, C. Saengow, et al., "Nano Oxygen Chamber by Cascade Reaction for Hypoxia Mitigation and Reactive Oxygen Species Scavenging in Wound Healing," *Bioactive Materials* 35 (2024): 67–81.
20. S. C. Hsieh, C. S. Lai, C. H. Chang, et al., "Nitric Oxide: Is It the Culprit for the Continued Expansion of Keloid?," *European Journal of Pharmacology* 854 (2019): 282–288.
21. J. Zhang and Q. Zhang, "VHL and Hypoxia Signaling: Beyond HIF in Cancer," *Biomedicine* 6, no. 1 (2018): 35–47.
22. J. K. Maranchie, J. R. Vasselli, J. Riss, et al., "The Contribution of VHL Substrate Binding and HIF1-Alpha to the Phenotype of VHL Loss in Renal Cell Carcinoma," *Cancer Cell* 1, no. 3 (2002): 247–255.
23. C. P. Martucci and J. Fishman, "P450 Enzymes of Estrogen Metabolism," *Pharmacology & Therapeutics* 57, no. 2–3 (1993): 237–257.
24. N. J. Lakhani, M. A. Sarkar, J. Venitz, and W. D. Figg, "2-Methoxyestradiol, a Promising Anticancer Agent," *Pharmacotherapy* 23, no. 2 (2003): 165–172.
25. K. T. Peta, C. Durandt, M. B. van Heerden, A. M. Joubert, M. S. Pepper, and M. A. Ambele, "Effect of 2-Methoxyestradiol Treatment on Early- and Late-Stage Breast Cancer Progression in a Mouse Model," *Cell Biochemistry and Function* 41, no. 7 (2023): 898–911.
26. W. Huw, X. Huang, J. Li, et al., "2-Methoxyestradiol Inhibits Melanoma Cell Growth by Activating Adaptive Immunity," *Immunopharmacology and Immunotoxicology* 44, no. 4 (2022): 541–547.
27. I. S. Batth, S. B. Huang, M. Villarreal, et al., "Evidence for 2-Methoxyestradiol-Mediated Inhibition of Receptor Tyrosine Kinase RON in the Management of Prostate Cancer," *International Journal of Molecular Sciences* 22, no. 4 (2021): 1852–1869, <https://doi.org/10.3390/ijms22041852>.
28. P. Bastian, L. Konieczna, J. Dulski, et al., "2-Methoxyestradiol and Hydrogen Peroxide as Promising Biomarkers in Parkinson's Disease," *Molecular Neurobiology* 61, no. 1 (2024): 148–166.
29. S. P. Tofovic, X. Zhang, T. J. Jones, and G. Petruševska, "2-Methoxyestradiol Attenuates the Development and Retards the Progression of Hypoxia- and Alpha-Naphthylthiourea-Induced Pulmonary Hypertension," *Prilozi* 42, no. 1 (2021): 41–51, <https://doi.org/10.2478/prilozi-2021-0003>.
30. C. Liu, X. Zhou, J. Lu, L. Zhu, and M. Li, "Autophagy Mediates 2-Methoxyestradiol-Inhibited Scleroderma Collagen Synthesis and Endothelial-To-Mesenchymal Transition Induced by Hypoxia," *Rheumatology* 58, no. 11 (2019): 1966–1975.
31. F. Long, L. Si, X. Long, B. Yang, X. Wang, and F. Zhang, "2ME2 Increases Radiation-Induced Apoptosis of Keloid Fibroblasts by Targeting HIF-1 α In Vitro," *Australasian Journal of Dermatology* 57, no. 2 (2016): e32–e38.
32. A. C. Keller, J. Ma, A. Kavalier, K. He, A. M. B. Brillantes, and E. J. Kennelly, "Saponins From the Traditional Medicinal Plant *Momordica charantia* Stimulate Insulin Secretion In Vitro," *Phytomedicine* 19, no. 1 (2011): 32–37.
33. M. Korke, K. Ishino, Y. Kohno, et al., "DMSO Induces Apoptosis in SV40-Transformed Human Keratinocytes, but Not in Normal Keratinocytes," *Cancer Letters* 108, no. 2 (1996): 185–193.

Supporting Information

Additional supporting information can be found online in the Supporting Information section.